The Structure, Dynamics, and Energetics of a Simulated Easterly Wave

Ming-Sen Lin

Central Weather Bureau, Taipei, Taiwan, ROC

(*Manuscript received 13 March 1976, in revised form 7 April 1976*)

Abstract

A theoretical study on the structure, dynamics and energetics of a forced easterly wave has been made. The wave is generated by using a quasi-geostrophic model which incorporates an external diabatic heating. This heating has been formulated to represent the effects of cumulus convective heating, evaporational, and radiational cooling. The generated wave is characterized by a cold-cored trough in the lower half of the atmosphere which tilts eastward with height. A region of organized upward motions occurs east of the 900-mb trough. In the upper atmosphere, there is a warm anticyclone which is located about 800 km to the east of the surface trough. Analysis of the vorticity budget of the wave shows that the largest term is the local tendency, it is primarily the combined effect of the horizontal advection and the divergence terms. If the effect of cumulus transport is incorporated in the vorticity equation, the amplitude of the streamline pattern is decreased. The thermodynamic energy budget shows tnat the two dominant terms are the vertical advection and the diabatic terms. The easterly wave as a whole can maintain its kinetic energy by converting available potential energy to kinetic energy in the upper troposphere. Kinetic energy in this region is exported to the middle and lower troposphere by the pressure flux term.

I. Introduction

The existence of westward traveling wave disturbances in the trade wind easterlies and the easterlies of the equatorial trough region has been recognized since the early studies of Riehl (1945) and Palmer (1952). Riehl's studies show that the waves move westward at the rate of about 6 m sec^{-1}; the average wavelength is approximately 2,000 km and the period is 3 to 4 days. Organized upward motions occur east of the trough line; descending motions occur west of the trough line. The axis of the trough line tilts eastward with height in the troposphere, the slope is very small in the lower troposphere. The thermal structure shows that the disturbances are generally cold-cored.

Recently, by using compositing technique, Reed and Recker (1971) found a similar wave, but not exactly the same structure as Riehl's wave on the equatorial western Pacific. The most significant difference is in the vertical

motion field. Reed and Recker found that upward motons and rainfall occur directly over the trough instead of behind it. There are also differences in the temperature structure. Whereas the negative temperature anomalies occur along the trough line in Riehl's study, their results indicate that they occur further to the east of the trough.

Spectrum and cross-spectrum analyses have been employed to obtain objective descriptions of their characteristics. There exists a wide range in zonal wavelength which is apparently due to the existence of two types of wave modes contributing to oscillations with periods of 4 to 5 days (Chang et al. 1970). The first type with a wavelength range of 2,500 to 5,000 km is most prominent in the lower troposphere at the western Pacific stations. The second type of wave mode, with a wavelength range of 6,000 to 10,000 km, has its maximum amplitude in the upper troposphere. The axes of waves of this mode generally have a substantial tilt with height.

The observational studies described above show large geographic variations in the wave properties such as wave structure, wavelength, and wave speed; there are presumably due to corresponding variations in the Trades.

Yanai and Nitta (1967) found that the easterly wave has maximum upward motions located to the east of the axis at about the 500 mb level and its order is about 4 cm sec^{-1}. The analysis of the vorticity budget shows that the horizontal advection of vorticity and the effect due to convergence are primary causes of the local changes of vorticity in the lower troposphere. On the other hand, the vertical transport of vorticity and the twisting effect also contribute to the vorticity change in the upper troposphere.

Nitta (1972) calculated the energy budget of wave disturbances over the Marshall Islands. He found that the eddy available potential energy is generated by the heat of condensation and is transformed to the eddy kinetic energy in the upper troposphere centered at about 300 mb. At this level, the increase in kinetic energy is approximately balanced by a decrease due to divergence of pressure energy flux. The other terms of energy transformation are one or two orders of magnitude smaller than terms of generation and conversion of eddy available potential energy.

In this paper, we will describe the results of a theoretical study on the energetics and vorticity mechanisms of a numerical simulation of an easterly wave. The wave is generated by prescribing an external diabatic heating function which resembles the observed effects of condensation heating, evaporational cooling, and radiative cooling. The realism of the simulated easterly wave is confirmed by comparing its structure with observations. Then, using the computed structure, we calculated the various components of the vorticity and the energy budgets. The vorticity budget is examined in order to determine the important processes which contribute to changes in vorticity. Finally, the calculated energy budget, is cross-checked to determine the energy sinks and sources, as well as the energy transformation processes, which are important in the maintenance of the easterly wave.

II. The Numerical Model

Equations:

The numerical model which is a quasi-geostrophic model, the final set of predictive equations and relations in β coordinate are as follows:

$$\frac{\partial \nabla^2\psi}{\partial t} = -J(\psi, \nabla^2\psi + f) + f_0 \frac{\partial \omega}{\partial p} + F \qquad (1)$$

$$\pi\sigma\nabla^2\omega + f_0^2 \frac{\partial^2\omega}{\partial \phi^2} = f_0 \frac{\partial}{\partial p} J(\psi, \nabla^2\psi) - f_0\nabla^2[J(\psi,$$

$$\frac{\partial \psi}{\partial p})] + f_0\beta \frac{\partial}{\partial p}\frac{\partial \psi}{\partial x} + f_0 \frac{\partial F}{\partial p} - \frac{R}{C_P p}\nabla^2 Q \qquad (2)$$

$$T = -\frac{f_0 p}{R}\frac{\partial \psi}{\partial p} \qquad (3)$$

where ζ =relative vorticity

ψ=streamfunction

f =coriolis parameter

T=temperature

ω=pressure change following a parcal

F=frictional dissipation and horizontal diffusion

Q=diabatic heating source

$$\pi = \frac{R}{P}\left(\frac{P}{P_0}\right)^{R/C_P}$$

The determination of Q and F will be discussed later.

For the purpose of obtaining an idea about the moisture distribution in the simulated wave, we compute the specific humidity, q, by using the following equation:

$$\frac{\partial q}{\partial t} = -J(\psi, q) - \omega\frac{\partial q}{\partial p} + E \qquad (4)$$

Here E is the evaporation from the sea surface computed by means of a drag coefficient.

Vertical and horizontal structure

The quasi-geostrophic set of equations must be applied at different levels in the vertical. From 900 mb to 100 mb a 200 mb resolution is used. The horizontal grid is a square grid with a mesh size of 2.5° latitude. The grid extends from equator to 30° N in N−S and 60° longitude in E−W. The integration was done on a 2.5° square mesh without a map factor.

Boundary conditions

The east-west boundary conditions are cyclic. For any time, the value on the last column of the cyclic region is set equal to value on the first column. This boundary condition is used for all variables. North and south boundary conditions are rigid walls. Omega is set equal to zero at 1,000 mb and at 0 mb the north and south boundary values of streamfunction are constant in E−W and in time.

Initial condition

The initial conditions correspond to a geostrophically-balanced zonal flow whose streamfunction is given by

$$\psi(y,p) = \bar{\psi}(p) + u_0\Delta y \tanh\left(\frac{y-y_0}{\Delta y}\right) \times \tanh\left(\frac{p-p_3}{\Delta p}\right) \qquad (6)$$

where $\bar{\psi}$ corresponds to the standard tropical atmosphere. The subscripts "0" and "3" indicate values at the 15° N and at the 300-mb level respectiyely. U_0 is chosen as 10 m sec^{-1}. The above represents an east-west flow which is characterized by a jet centered at 15° N, which is easterly below 300 mb and westerly above.

Finite difference methods

Eqs. (1), (2), and (3) are evaluated using a finite differencing technique. All of the Jacobians, horizontal advection terms, are evaluated by use of the Arakawa (1966) Jacobian. This technique is used because it conserves kinetic energy, mean square vorticity and the average wave number over the domain of integration. This is important in preventing computational insability caused by aliasing. The vertical derivates are evaluated using a centered finite difference approximation. The Laplacian is calculated as a five point operator, the time differencing scheme is Matsuno predictor corrector scheme (Matsuno, 1966).

Friction

Skin friction is parameterized in the vorticity equation and the effect is made

proportional to a mean surface wind speed times the relative vorticity as follows:

$$F=\frac{C_D V}{h}\nabla^2\psi \qquad (5)$$

where C_D = drag coefficient, equal to 0.0001
V = a mean wind speed, use 10m sec^{-1}
h = mean thickness of the boundary layer, 2 km.

The frictional influences enter the vorticity equation as a primary effect that, as a result, weakens any circulation. The term in the omega equation will tend to cause upward motion where there is positive relative vorticity and downward where there is negative relative vorticity. In addition to the skin friction, we also incorporate the effect of internal friction. This is given by $K_h\nabla^2\psi$, where K_h is horizontal eddy diffusion coefficient.

Diabatic heating

In order to generate the easterly wave, a diabatic heating function is specified. The function is given by:

$$Q(x,y,p,t)=Q_o h(p)\ \exp\left[-\left(\frac{y-y_o}{a}\right)^2\right] \times F(x-ct) \qquad (7)$$

where y_o = 15° N latitude
y = latitude of each grid point
a = 5° of latitude

$$F(x-ct)=0.248\cos\psi+0.224\sin\psi+0.020\cos2\psi+0.266\sin2\psi-0.130\cos3\psi+0.158\sin3\psi-0.145\cos4\psi+0.020\sin4\psi-0.075\cos5\psi+0.056\sin5\psi-0.011\cos6\psi-0.039\sin6\psi$$

where $\psi=\frac{2\pi}{L}(x-ct)$

L = 30° of latitude
c = propagation speed of heating wave.

and $h(p)=\sin^2\alpha-\sin\alpha$

where $\alpha=\left(\frac{p_o-p}{p_o}+0.15\right)\pi$

p_o = 1,000 mb

The diabatic heating is assumed to be a wave function in the east-west direction. Its primary wavelength of 30° latitude compares resonably with the observational results. The heating wave moves westward at a speed of 5° per day in the Control Experiment. The coefficient of each periodic function is chosen such that the total amount of heating is equal to that of cooling, therefore, there is no net heating in the domain of integration. We select a heating profile along the y direction which is a Gaussian function centered at 15° N. The function h(p), is the vertical distribution of diabatic heating. Finally, Q_o is a constant, is set equal to -6×10^5 °C sec^{-1}, so that we have a maximum heating of about 10°C per day. Eq. (7) represents a westward propagating heat wave whose space distribution is depicted in Fig. 1. and Fig. 2.

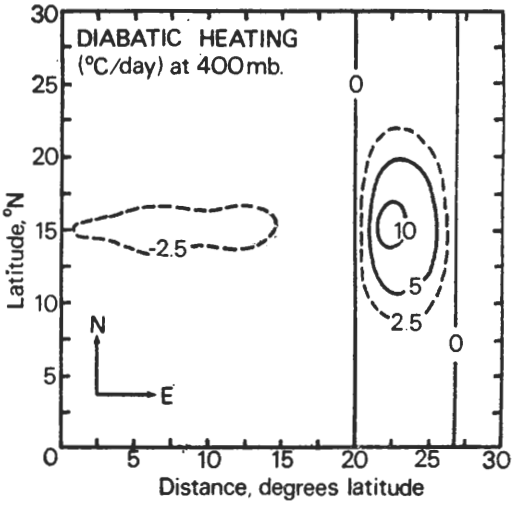

Fig. 1. Distribution of the diabatie heating at the level of maximum heating (400mb). Units, °C/day.

From Fig. 1, we find that the heating wave is cyclic along the E−W direction with a wavelength equal to 30° of latitude. Fig. 2 indicates the variation of the heating along the vertical through the region of maximum heating. The strong heating at

upper levels represents the heating by deep cumulus convection in the trough of easterly waves cited by Reed and Recker (1971) and Yanai et al. (1973), while the cooling in the lower troposphere represents evaporation cooling as suggested by Riehl (1967).

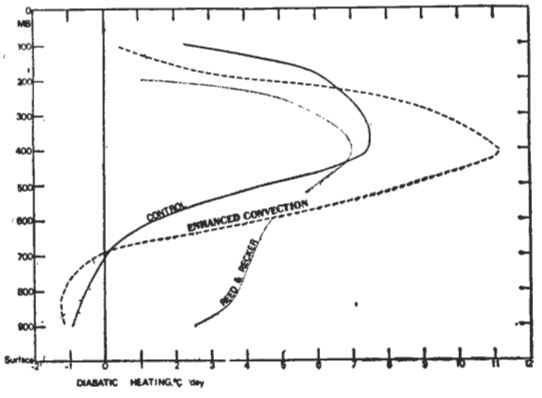

Fig. 2. Vertical profile of the diabatic heating near the region of maximum heating. Units, °C/day.

III. Design of the Numerical Experiments

The integrations have been made in order to determine the effects of certain factors in the structure, dynamics, and the energetics of disturbances. The factors are the vertical wind shear, speed of propagation of diabatic heating wave, and vertical distribution of heating source. We made five seperate integrations or experiments of the model. The first of these experiments is designed as the Control Experiment because it differs from any of the rest in only one aspect. Table 1 summarizes the characteristics of each experiment. The integrations for all experiments were carried out for 16 days of meteorological time, but diabatic heating has been removed after 8 days to examine the self-maintenance of free waves.

Table 1. Characteristics of the Numerical Experiments

Exp No.	Basic flow	Speed of heating	h(p)at 200, 400, 600, 800 mb level
1 (Control)	with vertical shear	5° day^{-1}	1.6, 2.0, 0.4, -0 1
2	no vertical shear	5° day^{-1}	1.6, 2.0, 0.4, -0.1
3	with vertical shear	7.5° day^{-1}	1.6, 2.0, 0.4, -0.1
4	with vertical shear	5° day^{-1}	1, 3, 1, -0.3
5	with vertical shear	5° day^{-1}	0.3, 2.7, 1.8 ,1.5

IV. The Control Experiment

The wave structure

The equations were integrated numerically, starting from the undisturbed zonal flow described above. The diabatic heating generated a wave disturbance as expected whose amplitude became more or less constant after about 8 days;after the eighth day, we removed the heating in order to examine the self-maintenance of free waves.

Fig. 3 shows the streamfunction and temperature distribution at low levels at 8 days. Fig. 4 depicts the horizontal profile of streamfunction, temperature, specific humidity, and upward motions at various lavels at this time.

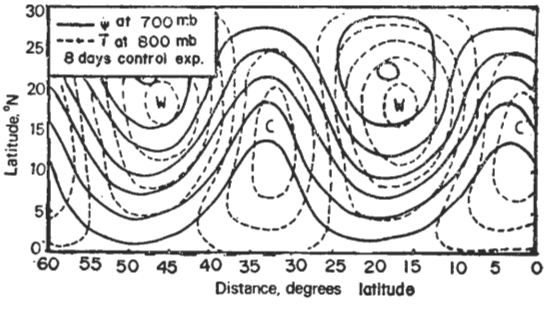

Fig. 3. Streamfunction and temperature distributions at t=8 days, respectively. Streamfunction contour interval, 10^6 m^2 sec^{-1} ; temperature contour interval, 0.4°C.

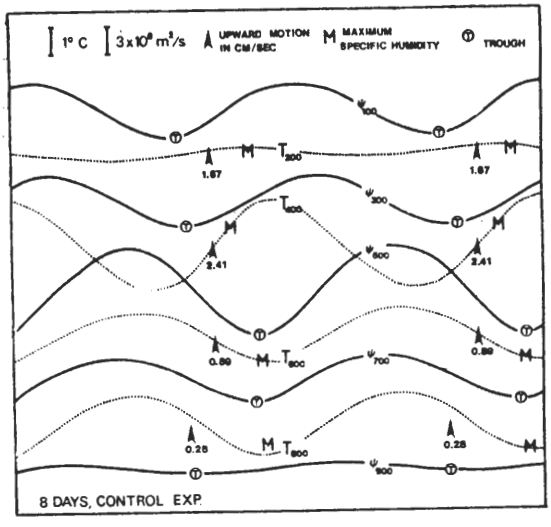

Fig. 4. The horizontal profile of streamfunction, temperature, specific humidity, and upward motions at various levels for the Control Experiment at t=8 days.

It may be recognized that the wave resembles the classical easterly wave presented by Riehl (1945) which we described in the Introduction section. The trough is weak at 900 mb and increases in intensity with height as indicated by the 700-mb trough. The trough axis tilts eastward with height until the 500-mb level, then westward above. The cold core of the low-level troposphere low stands out rather distinctly as shown in Fig. 4. The temperature pattern of the lower troposphere at 800 mb shows colder air in the 700-mb trough and somewhat warmer air ahead of the wave. By looking at Fig. 4 one can find out that the organized upward motions occur behind the 900-mb trough axis. The maximum speed of the upward motion is about 2.5 cm sec^{-1}. This location conforms with the usual observations of a region of convection associated with bad weather behind easterly wave troughs.

During the course of the integration we noted a dry region ahead of the easterly wave. The maintenance of a strong moisture gradient is primarily attributed to descending motions ahead of the easterly wave and vertical upward flux of moisture behind the wave axis.

After 8 days, we removed the diabatic heating, and the wave structure changed gradually with time. From Fig. 5, we can find that there is cold-cored in the lower troposphere with a temperature range of 1.2°C, and the trough is still weak at the 900-mb level but more pronounced at upper levels. The trough axis titls eastward with height to 700-mb level, then a little westward above. One also can find the upward motion is one order of magnitude smaller than the forced wave, and the organized upward motions are not apparent. Although the motion field changed slightly, the moisture field has changed considerably.

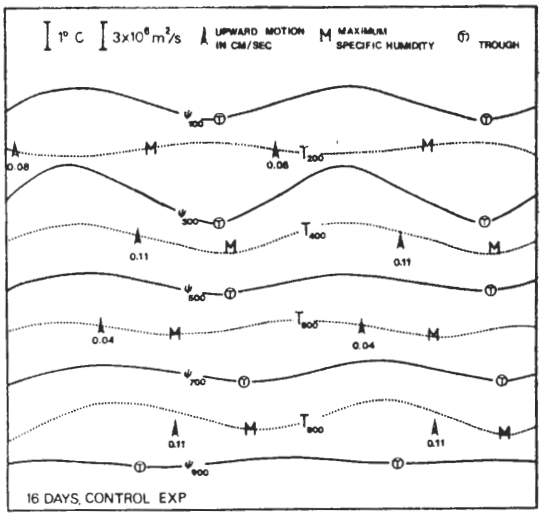

Fig. 5. The horizontal profile of streamfunction, temperature, specific humidity, and upward motions at various levels for the Control Experiment at t=16 days.

Vorticity budget

The vorticity equation can be written as:

$$\frac{\partial\zeta}{\partial t}=-\mathbb{V}\cdot\nabla\zeta-\beta v-f_0\nabla\cdot\mathbb{V}+k_h\nabla^2\zeta-\frac{C_D V}{h}\zeta_s \quad (8)$$

The subscript "s" indicates surface skin friction term (included only at 900-mb level), k_h the horizontal coefficient of diffusion is chosen as $10^5 m^2 sec^{-1}$. The terms of the vorticity equation at the 700-mb level are shown in Fig. 6 and Fig. 7. It may be seen that the local vorticity tendency is the largest term, representing the combined contribution of the horizontal advection and divergence terms.

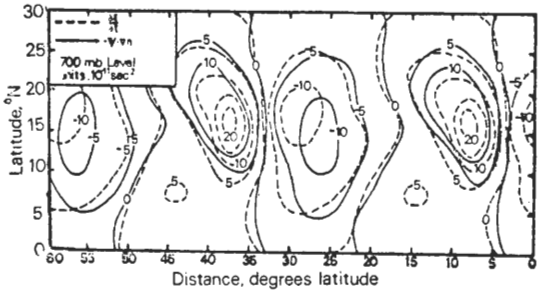

Fig. 6. Distributions of the vorticity advection and the local tendency at the 700-mb level for the Control Experiment at t=8 days. Units, 10^{-11} sec^{-2}.

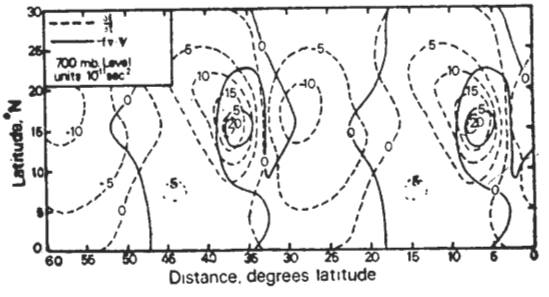

Fig. 7. Distributions of the divergence term and the local tendency at the 700-mb level for the Control Experiment at t=8 days. Units, 10^{-11} sec^{-2}.

From the corresponding terms at the 300-mb level, we note that the same additive effects of the horizontal advection and the divergence terms are contributing to local vorticity tendency which is the largest term in vorticity budget. The results of our study agrees quite well with Lateef's observational study (1967). Recently, Reed and Johnson (1974) calculated the vorticity budget of easterly wave disturbances in the tropical western Pacific by using the residual method with the aid of a composited structure. The conclusions of their analysis show that the cumulus transpot term and divergence term are two major components in the vorticity budget. The results of Reed and Johnson (op. cit.) and williams (1970) suggested that cumulus convective transport of vorticity must be incorporated in models of tropicl wave disturbances. Surprisely, Holton (1971) and Krishnamurti et al. (1973) were able to produce realistic results even though these models did not incorporate the cumulus convective transport of vorticity momentum.

In order to test the effect of cumulus transport on the structure of the perturbation, we modified the model by incorporating a cumulus transport term. Two cases were integrated. In the first case, (moderate convective transport), the ratio between the cumulus transport term to the divergence term (r) is equal to 0.5; in the second case (strong convective transport), r=0.9. It may be recognized that the amplitude of the streamlines for the case with moderate cumulus transport are smaller than those for the case without cumulus transport. Note also that the corresponding amplitudes for the case with strong cumulus transport are much smaller.

Thermodynamic energy budget

In this section we will discuss the thermodynamic energy budget, the equation can be written as:

$$\frac{\partial\theta}{\partial t}=-\mathbb{V}\cdot\nabla\theta+\omega\sigma+Q \quad (9)$$

We calculated the values of the different terms of this equation and plotted them in Fig. 8 which shows the results for the region over the surface trough.

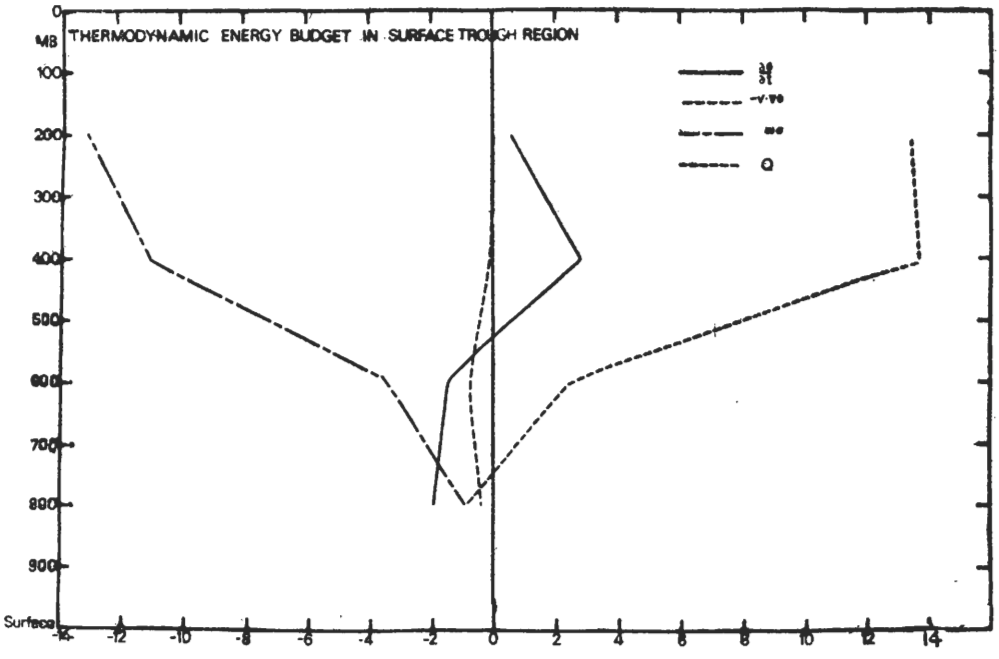

Fig. 8. Vertical profile of the thermodyamic energy budget over the surface trough. Units, 10^{-5} °C/day

In summary, the vertical advection term and the diabatic heating terms are most important at upper levels, but gradually decrease in their importance as one goes downward to the lower troposphere. This agrees with detailed scale analysis for tropical motions by Holton (1972) at middle and upper levels. However, at lower levels, the results of his scale analysis is not supported by our study.

Energy budget

From the model equations described in the former section, one can derive a quasi-geostrophic set of energy equations for the easterly wave which are:

$$\frac{\partial}{\partial t}(K'_{4,5}) = \frac{1}{A}\int_A \left[\bar{u}_5 \frac{\partial}{\partial y}\overline{(u_5'v_5')} + \bar{u}_4 \frac{\partial}{\partial y}\overline{(u_4'v_4')}\right] dA - \frac{f_o}{\Delta p}\frac{1}{A}\int_A \overline{(\psi_5'\omega_5' - \psi_4'\omega_3')}\, dA + \frac{f_o}{\Delta p}\frac{1}{A} \int_A \overline{\omega_4'\alpha_4'}\, dA - K_h \frac{1}{A}\int_A \overline{(\zeta_5'^2 + \zeta_4'^2)}\, dA - K_s \frac{1}{A}\overline{(u_6'u_5' + v_6'v_5')}\, dA \qquad (10)$$

$$\frac{\partial}{\partial t}(P'_{4\cdot5}) = -\frac{f_o^2}{\sigma g(\Delta p)^2}\frac{1}{A}\int_A \overline{v'\alpha'}\frac{\partial \bar{\alpha}}{\partial y} dA - \frac{f_o}{\Delta p}\frac{1}{A}\int_A \overline{\omega_4'\alpha'}\, dA + \frac{f_o^2}{\Delta p \sigma g}\frac{1}{A}\int_A \alpha' Q_4'\, dA - \frac{K_h f_o^2}{\sigma g(\Delta p)^2}\frac{1}{A}\int_A \overline{\nabla^2\alpha'}\, dA \qquad (11)$$

where $\alpha' \equiv \psi_5' - \psi_4'$

$\bar{\alpha} \equiv \overline{\psi_5} - \overline{\psi_4}$

$K' \equiv \frac{1}{2}(u'^2 + v'^2)$

$P' \equiv \frac{1}{A}\int_A \frac{f_o^2 \alpha'^2/2}{\sigma g(\Delta p)^2} dA$

The above equations are similar to the one derived by Phillips (1956). The subscript "4" or "5" indicates the level of data use at 800 and 900 mb. Similar equations may be derived for other levels. The operator $\frac{1}{A}\int_A (\quad) dA$ means that the energy is averaged in the whole domain (horizontal) of integration. The rest of the notation in standard use. We interpret the physical meaning of each term in the above equations. The left

side of Equation (10) represents the eddy kinetic energy tendency from 800 to 1,000 mb layer. The first term of right side indicates the transformation of zonal kinetic energy into the eddy kinetic energy or the barotropic term (denoted as $\{\bar{K} \cdot K'\}$). The second term represents the divergence of wave energy flux, sometimes this is called the pressure flux term. The third term is the energy conversion from eddy available potential energy to eddy kinetc energy or the baroclinic term (denoted as $\{P' \cdot K'\}$). The fourth term indicates the loss of eddy kinetic energy by lateral eddy-viscosity denoted as $\{K' \cdot A\}$. Finally, the loss of kinetic energy by skin friction is denoted by the last term. Eq. (11) may be interpreted in a similar manner. The left side of this equation represents the time rate of change of eddy potential energy from 800 to 1.000 mb layer. The first term of the right side of this equation repersents transformation of the zonal potential energy into the eddy potential energy (denoted as $\{\bar{P} \cdot P'\}$). The second term is the baroclinic term. The third term represents the generation of eddy potential energy by eddy diabatic heating (denoted as $\{Q' \cdot P'\}$). And the last term represents the tendency of the horizontal diffusion process to smoothe out the temperature gradients (denoted ns $\{P' \cdot A\}$).

An interesting way of presenting these various energy transformations is in the form of an energy flow diagram. The bracketed quantities then represent the "flow" of energy, their form being given by the expressions above. We are mainly interested in the budgets of eddy kinetic and eddy potential energy.

We have analyzed the energetics of the easterly wave during two stages of development—the active stage and the dissipative stage. The active stage occurs during the period t=0 to t=8 days of the integration. During the 8-day period after t=8 days, the diabatic heating was set equal to zero. Hence there was no longer an external energy source so that it is appropriate to call this peroid as the dissipative stage.

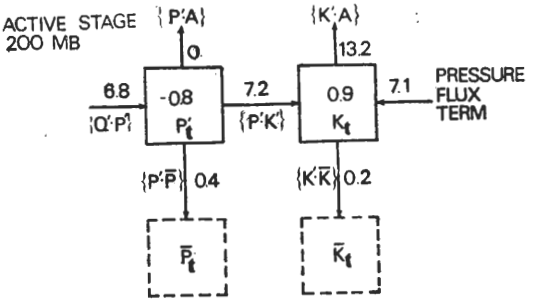

Fig. 9. The energy budget (Control Experiment) during the active stage for the 200-mb level. Units, 10^{-6} m^2 sec^{-3}.

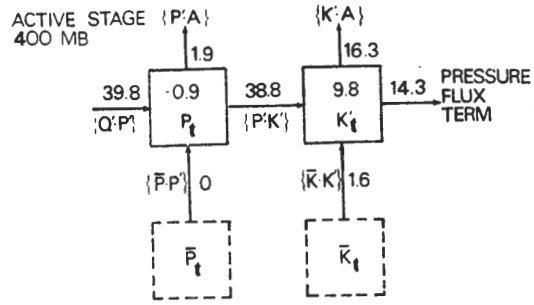

Fig. 10. The energy budget (Control Experiment) during the active stage for the 400-mb level. Units, 10^{-6} m^2 sec^{-3}.

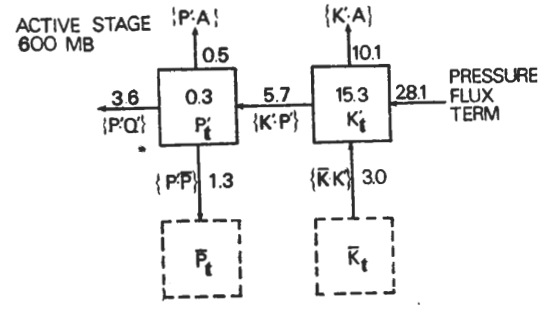

Fig. 11. The energy budget (Control Experiment) during the active stage for the 600-mb level. Units, 10^{-6} m^2 sec^{-3}

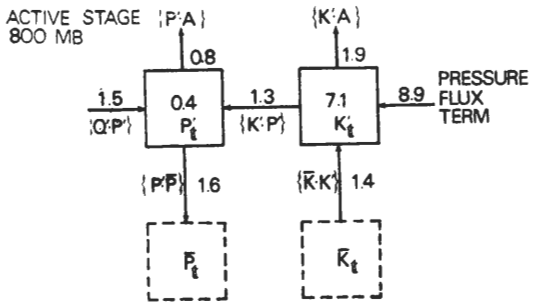

Fig. 12. The energy budget (Control Experiment) during the active stage for the 800-mb level. Units, 10^{-6} m^2 sec^{-3}.

In summary, the results show that the major components of the energy are the eddy diabatic heating term, the pressure flux term, the diffusion of the eddy kinetic energy term and the conversion term between the eddy potential energy and the eddy kinetic energy. The results also are in substantial agreement with the observational study by Nitta (1972) over the Marshall Islands. The simulated easterly waves are characterized by an indirect circulation in the lower and middle troposphere. Thus, kinetic energy is converted into available potential energy in these regions. We recall that the wave is warm-cored in the upper troposphere where the air is rising. Therefore, kinetic energy is generated from available potential energy in this layer. Hence, the easterly wave as a whole can maintain its kinetic energy in steady state by producing enough kinetic energy in the upper troposphere to counteract frictional dissipation and the kinetic energy consumption by the indirect cell in the lower and the middle troposphere. In order to prevent the continuous increase of kinetic energy in the region of generation (upper troposphere) and its decrease in the region of consumption (lower and middle troposphere), kinetic energy must be exported from the former to the latter. The process which appears to do this is the pressure flux term. Next, we consider the maintenance of the available potential energy. We note that this energy tends to decrease in the upper troposphere due to its conversion into kinetic energy. In order to counteract this decrease, the system creates available potential energy through diabatic heating. We note also that, in the middle troposphere, available potential energy tends to increase as a result of kinetic energy conversion. The decrease of avilable potential energy appears to be accomplished by loss due to both diabatic effects, transformation into mean available potential energy. In the lower troposphere, the available potential energy tends to increase as a result of the eddy kinetic energy conversion and the diabatic term. In order to counterbalance this effect, the eddy available potential energy decreases due to transformation into mean available potential energy and horizontal diffusion.

The energy budget for dissipative stage is much different from the wave diabatic heating. We note that, at this stage, the generation of eddy available potential energy is identically zero. The conversion term from the eddy potential energy is also very small. As expected, the eddy kinetic energy tendency is negative at all levels. The decrease of the eddy kinetic energy reaches its maximum at the middle level. $\{K' \cdot A\}$ and the pressure flux term are two major factors which contribute to the eddy kinetic energy tendency. Other terms of energy transformation such as $\{K' \cdot \bar{K}\}$, $\{P' \cdot \bar{P}\}$ and the diffusion term $\{P' \cdot A\}$ are relatively small compared to $\{K' \cdot A\}$ and the pressure flux term.

V. Other Experiments

This section discusses various factors which may affect the occurrence and the behavior of wave disturbances. The factors which are considered are the vertical wind shear, the speed of propagntion of the diabatic heating wave, and the vertical distribution of heat sources,

Experiment No. 2 has been designed to determine the role of the vertical wind shear of the basic flow in the structure, dynamics. and the energetics of disturbances. We find that the wave structure resembles that of the Control Experiment in the lower troposphere. However, in the upper troposphere, the warm anticyclone is located just over the warmest area instead of being shifted to the east. From the vorticity budget, we note that the local vorticity tendency is the largest term at all levels representing the combined contribution of the horizontal advection and divergence terms. In summary. this experiment has shown that the vertical wind shear changes the thermal structure. However, it does not affect significantly the dynamics of the easterly wave, The most interesting feature is concerned with the energetics. The result shows that the characteristics of this experiment resembles the Control Experiment in the middle and lower troposphere, but the magnitudes of the terms are much larger than those of the Control Experiment.

Experiment No. 3 was intended to determine the effect of the heating wave. This is done by replacing the westward propagating speed from 5°/day to 7.5°/day. One can find that the amplitude of the wave in the streamfunction and temperature field is much smaller than that of the Confrol Experiment. This may be explained by the fact that, in this experiment, the wave travels faster than the average speed of the basic easterly current and, also the corresponding Rossby wave. The upward motions are to the west of the surface trough, This result is supported by Riehl's study (1967). The vorticity budget shows that, the local tendency is the largest term at all levels, representing mainly the contribution from the divergence term. From the thermodynamic energy budget, the balance between the vertical advection term and the diabatic heatiag term applies to all levels. This confirms the study by Holton (1972). By comparing with the corresponding energy budgets. we find that the magnitude of each term is much smaller than those of the Control Experiment. It implies that the fast-moving wave cannot transform the energy efficiently.

In experiment No. 4, the intensities of the low-level cooling and the upper-level warming are increased, so the experiment simulates the effect of enhanced convection. By comparing this experiment with the Control one, we find that the waves are more perturbed in the lower troposphere. However, not much change occurs in the middle and upper troposphere. From the vorticity budget, we note that the magnitude of the vorticity tendency which is the largest term is much larger than that of the Control Experiment at the lower levels. For the thermodynamic energy budget, similar characteristics as those of the Control Experiment can be recognized. In summary, the simulated waves for the enhanced convection and no vertical wind shear experiments show the same characteristic of having large values of the eddy kinetic energy tendency at all levels.

Finally, Experiment No. 5 is an attempt to simulate an easterly wave by using Reed's heating profile (see Fig. 2)(op. cit.). As mentioned before, his profile lacks the cooling by evaporation at low levels. We can find that the most significant difference is the thermal structure in the lower troposphere. The wave is primarily warm-cored at the central latitude. From this experiment, we conclude that the low-level cooling is indispensable in producing the cold core in an easterly wave. In summary, due to the diabatic heating both at the lower and middle levels, the easterly wave gains its kinetic eneggy at this two levels by conversion from available potential energy. This process is reflected as a large amplitude in the streamfuntion.

VI. Summary and Conclusions

In this paper, we described the results of a theoretical study on the structure, dynamics, and energetics of a forced easterly wave based on a quasi-geostrophic model. The weve is generated by prescribing an external diabatic heating function which resembles the observed effects of condensation heating, evaporational cooling, and radiative cooling. We found that with this model, it may be possible to simulate an easterly wave which is realistic. Based on the Control Experiment, which does not incorporate the effects of cumulus vorticity transport, we note that the local tendency is the largest term, representing the combined contribution of the horizontal advection and divergence terms. Incorporating the effects of cumulus vorticity transport in the model, the most apparent change is to decrease the perturbation in the streamline pattern. This condition may explain the fact that intense weather activity is sometimes observed on weather maps even when tropical waves are characterized by very weak cyclonic curvatures in the horizontal flow field. As far as the thermodynamic energy budget is concerned, we found that the vertical advection term and the diabatic heating term are most important in the middle and upper troposphere. However, in the lower troposphere, this is not the case. From the energy budget, we found that the easterly wave can maintain its kinetic energy in steady state by producing kinetic energy in the upper troposphere, where the wave is warm-cored, to counteract frictional dissipation and the kinetic energy consumption by the indirect cell in the lower and the middle troposphere. Kinetic energy is converted into available potential energy in the lower and middle troposphere. In order to prevent the continuous increase of kinetic energy in the upper troposphere, kinetic energy is exported to the middle and lower troposphere by the pressure flux.

by comparing the results of additional experiments with those of the Control Experiment, we obtained some other important conclusions. We note that the vertical wind shear changes the thermal structure, but it does not affect significantly the dynamics of the easterly wave. It could be inferred that, for the same heating, the wind shear tends to decrease the amplitude of the wave.

For the wave which travels faster than the average speed of the basic easterly current and the corresponding Rossby wave, the upward motions are to the west of the surface trough. The faster the wave moves westward, the further ahead the bad weather is shifted.

The simulated waves for the enhanced

convection and no vertical wind shear experiments show the same characteristic of having large values of the eddy kinetic energy tendency at all levels. It appears that if the model does not incorporate the effect of evaporation cooling at lower levels, the wave cannot be cold-cored in the lower troposphere. Therefore, we conclude that the low-level cooling is indispensable in producing the cold-cored of an easerly wave.

Acknowledgments

Much appreciation is dut to Professor Mariano Estoque for his constant guidance and encouragement throughout this study, without which this work would never have been completed. I would like to express my appreciation to Dr. Lawrence Lahiff for his help in the numerical model and many useful comments. Professor Claes Rooth also contributed many helpful suggestions. This study was Supported by the National Science Council of the Republic of China.

References

Arakawa, A., 1966: Computational design for long term numerical integration of the equations of motion: two-dimensional incompressible flow, Part 1. *J. Comp. Phys.*, 1, 119-143.

Chang, C. P., V. F. Morris, and J. M. Wallace, 1970: A statistical study of easterly waves in the western Pacific July - Dec. 1964. *J. Atmos. Sci*, 27, 195-201.

Estoque, M. A., M. S. Lin, and L. N. Lahiff, 1975: Vorticity budget of the easterly wave in relation to cumulus transport. Paper to be submitted to *J. Atmos. Soi.*,

Holton, J. R., 1970: A note on forced equatorial waves. *Mon. Wea. Rea.*, 98, 614-615.

Holton, J. R., 1971: A diagnostic model for equatorial wave disturbances: the role of vertical shear of the mean zonal wind. *J. Atmos. Sci.*, 28, 55-64.

Holton, J. R., 1972: *An introduction to dynamic meterology*. Academic press New York and London, pp 319.

Jordan, C. L., 1958: Mean soundings for the West indies area. *J. Meteor.*, 15, 91-97.

Krishnamurti, T. N., and M. Kanamitsu, 1973: A study of a coasting easterly wave. *Tellus*, 25, 568-585.

Lateef, M. A., 1967; A case study concerning vertical motion, divergence, and vorticity in the troposphere over the Caribbean. *Mon Wea. Rev.*, 95, 778-790.

Matsuno, T., 1966: A finite difference scheme for time integrations of oscillatory equations with second order accuracy and sharp cut-off for high frequencies. *J. Meteor. Soc. Japan*, 44, 85-88.

Nitta, T., 1972: Energy budget of wave disturbances over the Marshall Islands during the years of 1956 and 1958. *J. Met. Soc. Japan*, 50, 71-83.

Phillips, N. A., 1956: The general circulation of the atmosphere: a numerical experiment. *Quart. J. Royal Met. Soc.*, 82, No. 352.

Palmer, C. P., 1952: *Tropical meteorology. Quart. J. Royal Met. Soc.*, 78, 126-163.

Reed, R. J., and E. E. Recker, 1971: Structure and properties of synoptic scale wave disturbances in the equatorial western Pacific. *J. Atmos. Sci.*, 28, 1117-1133.

Reed, R. J., and R. H. Johnson, 1974: The vorticity budget of synoptic-scale wave disturbances in the Tropical Western Pacific. *J. Atmos. Sci*,, 31, 1784-1790.

Riehi, H., 1945: Waves in the easterlies and the polar front in the tropics. Misc. rept. No. 17 Dept of Meteorology, Uni. of Chicago. pp 79.

Riehl, H., 1967: Varing structure of waves in the easterlies. International proceedings of the symposium on the dynamics of large-scale. Atmospheric Process, Moscow, 411-416.

William, M. G., 1970: A statistical analysis of satellite-observed trade wind cloud clusters in the western north Pacific. Atmos. Sci. paper No. 161, Colorado state Uni.

Yanai, M., and T. Nitta, 1967: Computation of vertical motion and vorticity budget in a Caribbean easterly wave. *J. Meteor. Soc. Japan*,

45, 444-466.

Yanai, M., S. Esbensen, and J. Chu, 1973: Determination of average bulk properties of tropical cloud clusters from large-scale heat and moisturc budget. . *Atmos. Sci.*, 30, 611-627.

模擬東風波之結構、動力平衡與能量收支

林 民 生

中央氣象局

摘 要

本文應用準地轉風模式模擬東風波，研究其結構、動力平衡與能量收支；此項非絕熱效應代表凝結加熱，蒸發及輻射冷却。模擬產生之波動在對流底層爲冷心型槽線，並隨高度向東傾斜，上升氣流區位於900 mb 槽線之東；在對流上層則轉爲暖性反氣旋。渦旋方程式中，渦旋的當地趨勢項爲最大，此項由水平渦旋平流和輻散項所共同合成。假設模式中包含積雲渦旋傳送效應，最顯著之差異爲擾動的流線型式減弱。至於熱力能量平衡方面，則以垂直方向之平流項和非絕熱項爲最重要。從能量收支的觀點來探討，發現東方波可以維持其平衡，此爲對流上層之位能轉換爲動能，而動能則自高層經由壓力通量項輸送至中，低大氣層。